Proceedings of the Institution of Civil Engineers
Structures & Buildings 158
February 2005 Issue SB1
Pages 21–40

Paper 13310
Received 14/03/2003
Accepted 08/09/2003
Keywords:
building structure & design/ concrete structures/seismic engineering

Francis T. K. Au
Associate Professor, The University of Hong Kong, Pokfulam Road, Hong Kong, China

Kun Huang
Former Research Student, The University of Hong Kong, Pokfulam Road, Hong Kong, China

Hoat J. Pam
Associate Professor, The University of Hong Kong, Pokfulam Road, Hong Kong, China

ice

Diagonally-reinforced beam–column joints reinforced under cyclic loading

F. T. K. Au PhD, MSc, CEng, RPE, MICE, MIStructE, MHKIE, K. Huang PhD, MEng and H. J. Pam PhD, ME, Ir, MHKIE, MIEAust, MIPENZ, CPEng

The beam–column joints in a reinforced concrete frame are vulnerable to damage caused by seismic events. The conventional detailing using transverse hoops usually results in serious joint congestion, which creates contruction problems. This paper introduces a new detail especially developed for low to medium seismicity, which involves the use of additional diagonal bars in the joint. Six half-scale interior beam–column assemblies with different joint details, namely 'empty', nominal transverse reinforcement and diagonal bars, tested under reversed cyclic loading are reported. The empty joint is not suitable even under moderate seismicity. The test results show that the joints containing the newly proposed detail, with or without axial compressive load present in the column, exhibit better behaviour at the lower range of ductility factors in terms of higher load-carrying capacity, greater stiffness and less strength degradation. Therefore, the newly proposed joint detail is suitable for beam–column joints of reinforced concrete buildings located in regions of low to medium seismic risk.

NOTATION

A_g	gross cross-sectional area of the column
A_{S1}	cross-sectional area of top beam reinforcement (Eurocode 8)
A_{S2}	cross-sectional area of bottom beam reinforcement (Eurocode 8)
A_{sd}	total area of diagonal steel bars in one direction
A_{sh}	cross-sectional area of transverse reinforcement in the joint (Eurocode 8)
b_j	effective joint width normal to the plane of beam–column joint
C_c	concrete compressive force acting on periphery of joint from beam (also C'_c)
C_s	steel compressive force acting on periphery of joint from beam (also C'_s)
D_c	compressive force carried by diagonal concrete strut
D_s	diagonal compression field in truss mechanism
e_1, e_2	readings of linear variable displacement transducers to evaluate joint distortion
f'_c	compressive cylinder strength of concrete (also f_{cd} according to Eurocode 8)
f_{cu}	compressive cube strength of concrete
f_y	yield strength of reinforcement (also f_{yd} according to Eurocode 8)
h_c	width of column in the direction of beam
h_{jc}	distance between reinforcement at two faces in column (Eurocode 8)
h_{jw}	distance between top and bottom reinforcement in beam (Eurocode 8)
L_b	distance between jacks 1 and 2
L_c	distance between top and bottom hinges for column
l_i	initial distance between mounting rods for LVDT for evaluation of joint distortion
M_n	nominal flexural strength of beam
P	compressive axial load applied to the column
P_1, P_2	forces applied by jacks 1 and 2 respectively
q	behaviour factor (Eurocode 8)
T	steel tensile force acting on periphery of joint from beam (also T')
V_c	column shear force
V_{jh}	joint shear (also V_{jhd} according to Eurocode 8)
V_{max}	measured equivalent shear strength of column
V_n	nominal shear strength of column derived from nominal flexural strength of beam
V_{sh}	bond force from the longitudinal reinforcement of beam
V_{sv}	bond force from the longitudinal reinforcement of column
v_d	normalized design axial force (Eurocode 8)
v_j	average shear stress in the joint core
β	initial inclination of LVDTs to horizontal (for evaluation of joint distortion)
γ_{Rd}	design value of overstrength ratio of steel (Eurocode 8)
Δ	peak displacement measured in the test
Δ_1, Δ_2	beam displacements at jacks 1 and 2 respectively (upward as positive)
Δ_c	column drift
ΔT_c	bond force of the part of longitudinal bars overlapping with the concrete strut
Δ_y	nominal yield displacement
η	drift ratio
η_u	ultimate drift ratio
θ	inclination of diagonal bars
λ	factor accounting for the available shear resistance

	of plain concrete after cyclic degradation (Eurocode 8)
μ	displacement ductility factor
μ_u	ultimate displacement ductility factor
ρ_h	volumetric ratio of the joint reinforcing steel in the loading direction
τ_{Rd}	basic design shear strength of member without shear reinforcement (Eurocode 8)

1. INTRODUCTION

Most tall buildings constructed of concrete can be categorised into two frame structures, shear wall structures and core wall structures. Although reinforced concrete (RC) frames appear in many diverse forms; their use as part of the structure or the primary structure is fairly common. In some regions of low to moderate seismicity, building structures are commonly designed primarily for the effects of dead load, live load and wind load while seismic risk is regarded as a secondary consideration. The earthquakes in Kobe (Japan, January 1995) and Izmit (Turkey, August 1999) have reminded us vividly of what can happen to a modern high-rise metropolis if there is insufficient forethought. Even if a region is not located in an active seismic zone, seismic risk still exists. Through the lessons learnt from past earthquakes and experimental research, engineers recognise that the seismic resistance of an RC structure hinges on how well its structural members have been detailed.

After years of study, it is recognised that the beam–column joint plays such an important role in ductile moment-resisting frames that its integrity should be ensured throughout the loading history.[1–3] The behaviour of a beam–column joint under earthquake load is so complex that the various national design approaches still differ to various degrees. A very significant measure in providing sound earthquake resistance is a properly detailed strategy. This can account for uncertainties in design and construction so that sufficient ductility for inelastic energy dissipation is achieved in the event of an earthquake. Ductility is actually a measure of the ability of a structure or structural member to undergo deformations of large amplitudes in the inelastic range without a substantial reduction in strength. An effective earthquake-resistant structure can be obtained by the proper design of the beam–column joints together with the adoption of the capacity design rationale.[4] However, in some regions of low to moderate seismic risk, the detailing of beam-column joints is not always accorded the necessary attention. For instance, in Hong Kong it is not necessary to design joints for seismic resistance under the commonly accepted codes.[5,6] Apart from the longitudinal bars along the beams and columns, the joints are often left 'empty' without any transverse reinforcement at all. The insufficient shear resistance may lead to non-ductile failure once the shear capacity of the concrete has been exceeded.

On the other hand, the detailing of beam–column joints of RC frame structures in regions of high earthquake risk is normally governed by code provisions[7,8] that require a considerable amount of transverse reinforcement to resist the horizontal joint shear forces, often resulting in extreme congestion. Although relaxation of such requirements is allowed under certain conditions, the congestion in beam–column joints still causes difficulties in fabrication of the steel reinforcement cage and adversely affects the placement of concrete within the beam–column joint. To ease the congestion, especially for joints of RC frame structures located in regions of low to moderate earthquake risk, a detail in the form of cross-diagonal reinforcement at the interior beam–column joints is proposed. The use of diagonal reinforcing bars in exterior beam–column joints has been studied[9] and the detail has been shown to be effective at improving the seismic resistance of such joints. Initial findings on the use of cross-diagonal reinforcement in interior beam–column joints have been rather promising.[10] This paper describes the detailed experimental investigation into the strength and ductility of interior beam–column joints with the proposed detail under moderate earthquake effects. Comparison is also carried out between the proposed detail, the empty joints and those with conventional transverse reinforcement.

2. FORCES IMPOSED ON AN INTERIOR BEAM–COLUMN JOINT

Under the action of lateral earthquake loading, a moment-resisting multi-storey multi-bay frame will deflect horizontally with points of contra flexure located roughly at the mid-length of the members. Figure 1(a) shows the deformation of a typical interior beam–column assembly. A typical interior beam–column joint is usually subjected to large shear forces due to lateral earthquake loading, as shown in Fig. 2. The bending moments and shear forces acting on the joint give rise to both horizontal and vertical shear forces at the joint core. The situation becomes critical under large cyclic reversals of ground shaking, possibly causing extensive damage to the joints.

In the ductile design approach, the frame is expected to undergo inelastic lateral displacements, with the beams forming plastic hinges adjacent to the column while the column is normally designed to remain elastic with the possible exception of beam–column joints and ground storey columns. It is essential that the beam–column joint is capable of transmitting the necessary shear forces across the joint core, which may have cracked. Figure 3 shows two commonly accepted mechanisms[3,7] postulated to explain the shear resistance of the joint core. In the strut mechanism, a diagonal concrete strut carrying a compressive force, D_c, is mobilised primarily by the concrete compressive forces denoted by the symbols, C_c, (with different number of primes) and bond forces, ΔT_c, (with different number of primes) of the part of longitudinal bars overlapping with the concrete strut. The maximum strength, D_c, of the strut mechanism is often associated with the horizontal and vertical joint shear resistances.[3] The truss mechanism essentially consists of a diagonal compression field, D_s, acting together with the vertical and horizontal reinforcement within the joint core. The bond forces, V_{sh} and V_{sv}, from the longitudinal reinforcement of the beam and column, respectively, are idealised as uniformly distributed shear flow. Depending on the amount of transverse reinforcement provided, the concrete in which the truss or strut mechanism occurs is confined, so that its strength is higher than that of the cover concrete, and by the time joint shear failure occurs, the cover concrete will have already spalled off the elements coming into the joint.

With cyclic reversals of ground shaking, bond deterioration along the longitudinal beam reinforcement progresses gradually as a result of the shear cracking in the joint and the

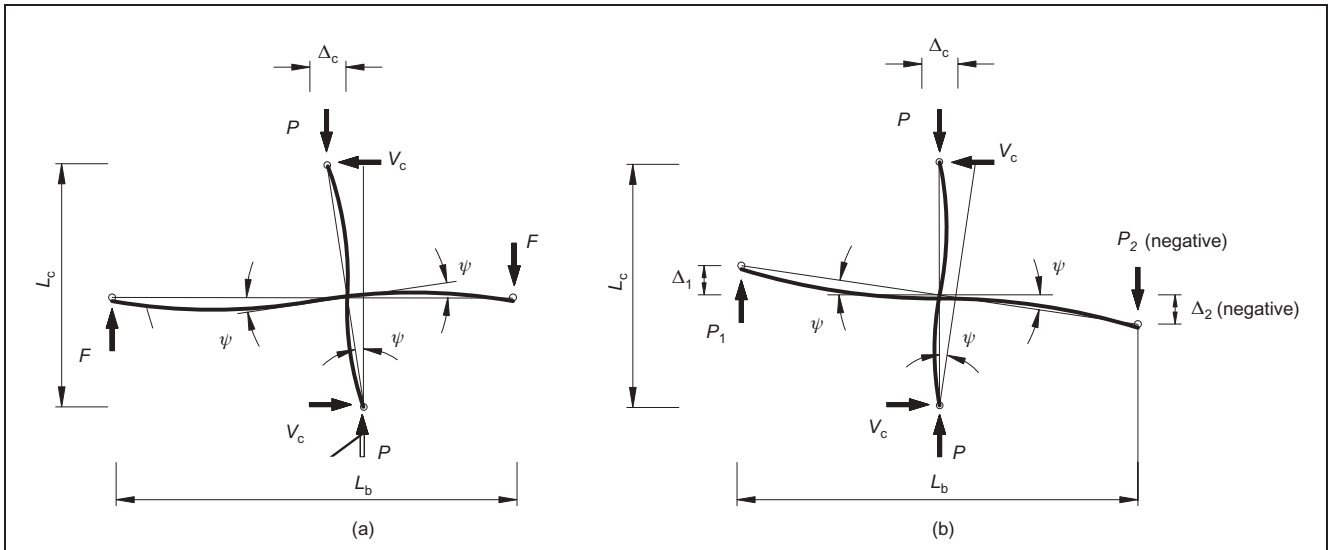

Fig. 1. Simulation of interior beam-column joint assembly by test specimen: (a) deformation of a typical interior beam–column joint assembly under lateral load; (b) assembly in loading rig

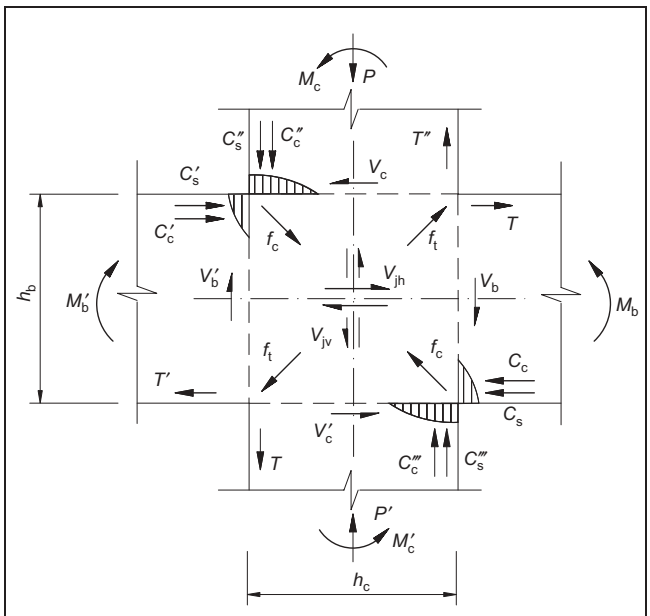

Fig. 2. Forces acting on the beam–column joint under seismic actions

increasing length of such reinforcement in the joint core that has yielded. The bending moments carried by the beams and columns create compressive forces acting on the periphery of the joint thus activating a concrete strut along a diagonal. As the strut compression increases together with bond deterioration, the contribution of the concrete strut may become significant while the resistance by the truss mechanism may diminish.[11,12] The reversed cyclic loading also weakens the concrete in the panel.[13] The joint shear failure is normally characterised by the eventual crushing of the concrete due to the compressive stress in the concrete strut.

3. EXPERIMENTAL PROGRAMME

3.1. Details of test specimens

To investigate and compare the behaviour of joint specimens with the proposed detail and other details, a number of half-scale beam–column joint specimens were fabricated and tested; this paper describes six of them. The beam–column assemblage represents a typical interior beam–column joint of a multi-storey frame bounded by the points of contra-flexure in the adjacent members. All the specimens were cast in concrete of specified characteristic cube strength f_{cu} of 40 MPa, and they had common cross-sectional dimensions of 250 × 300 mm for the beam and 300 × 300 mm for the column. The reinforcement details of all the specimens were identical, apart from the joints. The beam was equally reinforced at the top and bottom by four high-yield deformed bars of 16 mm diameter (i.e. 4T16) having specified characteristic yield strength f_y of 460 MPa, which are provided to cope with moment reversals. Stirrups bent from 6-mm-diameter mild steel round bars with specified characteristic yield strength of 250 MPa were provided at 130 mm centres (i.e. R6@130 stirrups). The column contained 16T16 longitudinal reinforcing bars evenly distributed around the perimeter. The transverse reinforcement in the column comprised R6 square hoops and R6 crossties in two perpendicular directions at 160 mm centres, as shown in Fig. 4.

The six specimens described in this paper consist of three pairs, namely the E-, H- and AD- series. The E-series (the 'empty' joint) contains no joint reinforcement apart from the longitudinal reinforcement of the beam and column. The specimens of this series serve as the reference specimens, as the detail is still adopted in some countries located in regions of low to moderate seismic risk. The H-series contains nominal transverse reinforcement in the form of hoops and crossties at the joint, whereas the AD-series contains additional diagonal bars as an alternative form of joint reinforcement. The specimens in each series have the same reinforcement details. One of them was tested with no axial force in the column that is, 0·0 in the specimen name. The other one was tested with an axial load level $P/f_{cu}A_g$ of 0·3 where P is the compressive axial load, f_{cu} is the cube strength of concrete and A_g is the gross cross-sectional area of the column, that is 0·3 in the specimen name.

Referring to Fig. 2, which shows the forces acting on a beam–column joint, the nominal horizontal shear force across the

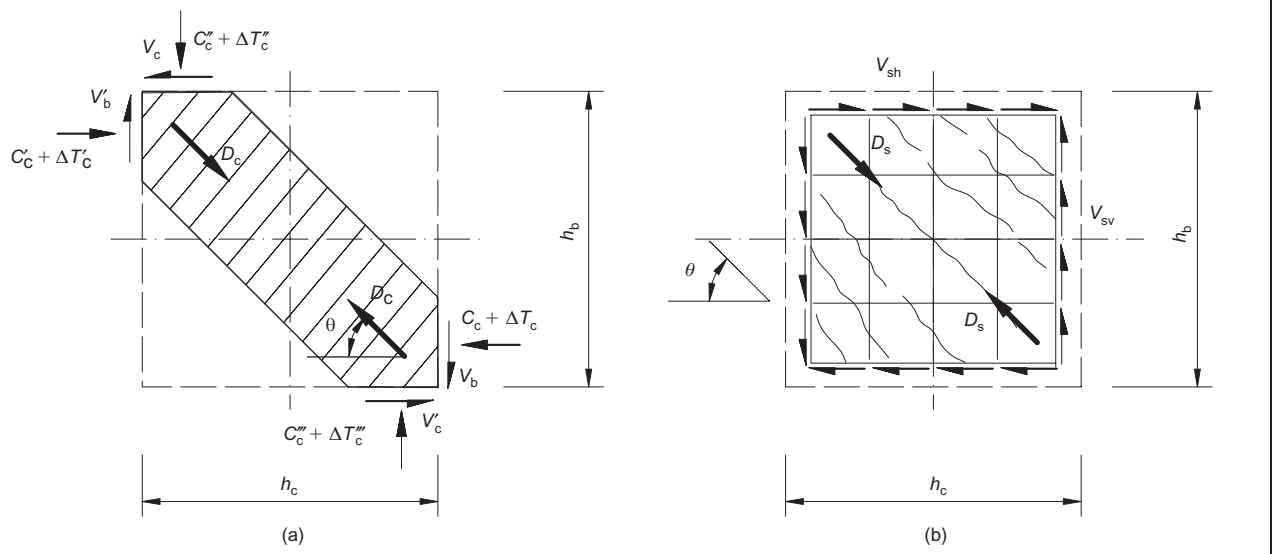

Fig. 3. Principal mechanisms of shear resistance of an interior joint core: (a) strut mechanism; (b) truss mechanism

joint V_{jh} can be obtained by considering the horizontal equilibrium of the upper part of the joint as

$$V_{jh} = C'_c + C'_s + T - V_c \quad (1)$$

where C'_c = concrete compression force on the upper left part of joint from beam; C'_s = steel compression force on the upper left part of joint from beam; T = steel tension force on the upper right part of joint from beam; and V_c = column shear force that may reach a value governed by the nominal flexural strength of beam with reference to Fig. 1.

The capacity design rationale,[4] strives to ensure a desirable hierarchy in the failure mode of a structure. This should not be based on the dependable capacities but rather on the most probable strengths of the structural components. In the present case, it is desirable that the beam fails flexurally but not otherwise. Therefore a frame is normally designed to have strong columns and weak beams. In addition, it is necessary to ensure that the dependable shear strength of the beam is not less than the shear force associated with the flexural overstrength of the beam. In the design of specimens, the flexural strength of the beam was evaluated in accordance with BS 8110,[6] one of the commonly used design codes in Hong Kong, taking all partial factors of safety as unity and treating it as a doubly reinforced section. Only the through longitudinal bars were considered even if additional diagonal bars were present. The self-weight of the beam was considered insignificant compared to earthquake loading, and hence it was ignored in the design. The flexural strength ratio of column to beam was about 1·5 without axial force or 2·2 with axial force such that flexural failure of the column is precluded as required by the capacity design approach. The cross-sectional area and spacing of stirrups in the beam and column were also designed to meet BS 8110.[6] The required shear force for the beam was obtained by dividing its bending moment capacity by the length of cantilever, while that for the column was derived from the equilibrium of the beam–column assembly.

Each joint of the H-series is provided with nominal transverse reinforcement comprising hoops and crossties, namely three sets of 3T12 (1018 mm^2), as shown in Fig. 4(b). The adequacy is checked against NZS 3101:1995[7] and Eurocode 8[14] for limited ductility requirements. However on checking against the requirements of NZS 3101:1995,[7] the transverse reinforcement provided satisfies neither the stated limit of $0{\cdot}2f'_c$ for the nominal horizontal joint shear stress v_{jh} (clause 11.4.3.2), nor the requirement of effective horizontal joint shear reinforcement A_{jh} (clause 17.3.8.3) when there is no column axial load. In particular, this code has allowed for the flexural overstrength as the tension reinforcement may attain a stress level above the yield stress under large deformations, which may subsequently cause a higher horizontal shear force in the joint. However the use of the overstrength factor does not appear really necessary for the case of moderate seismicity. For example, Eurocode 8[14] does allow certain relaxation in this respect. With regard to the required hysteretic dissipation capacity, three ductility classes (DC) are distinguished for concrete structures, namely DC 'L' (low ductility), DC 'M' (medium ductility), and DC 'H' (high ductility). The relevant requirements of DC 'M', which enable the structure to enter well within the inelastic range under repeated reversed loading without suffering brittle failure, are considered suitable for the case of moderate seismicity here. Eurocode 8[14] provides a simplified expression of the shear force acting on the concrete core of the joint V_{jhd} (clause 2.10.1.2) as

$$V_{jhd} = \gamma_{Rd}(2/3)(A_{S1} + A_{S2}q/5)f_{yd} - V_c \quad (2)$$

where γ_{Rd} = design value of overstrength ratio of steel (1·15 for DC 'M'); A_{S1} = cross-sectional area of top beam reinforcement (804 mm^2); A_{S2} = cross-sectional area of bottom beam reinforcement (804 mm^2); q = behaviour factor taken as 3·75 for RC frame; f_{yd} = design value of yield stress of steel (460 N/mm^2); and the reduction factor of two-thirds accounts for the part of the inclined bond forces flowing sideways out of the core of the joint. The diagonal compression induced by the

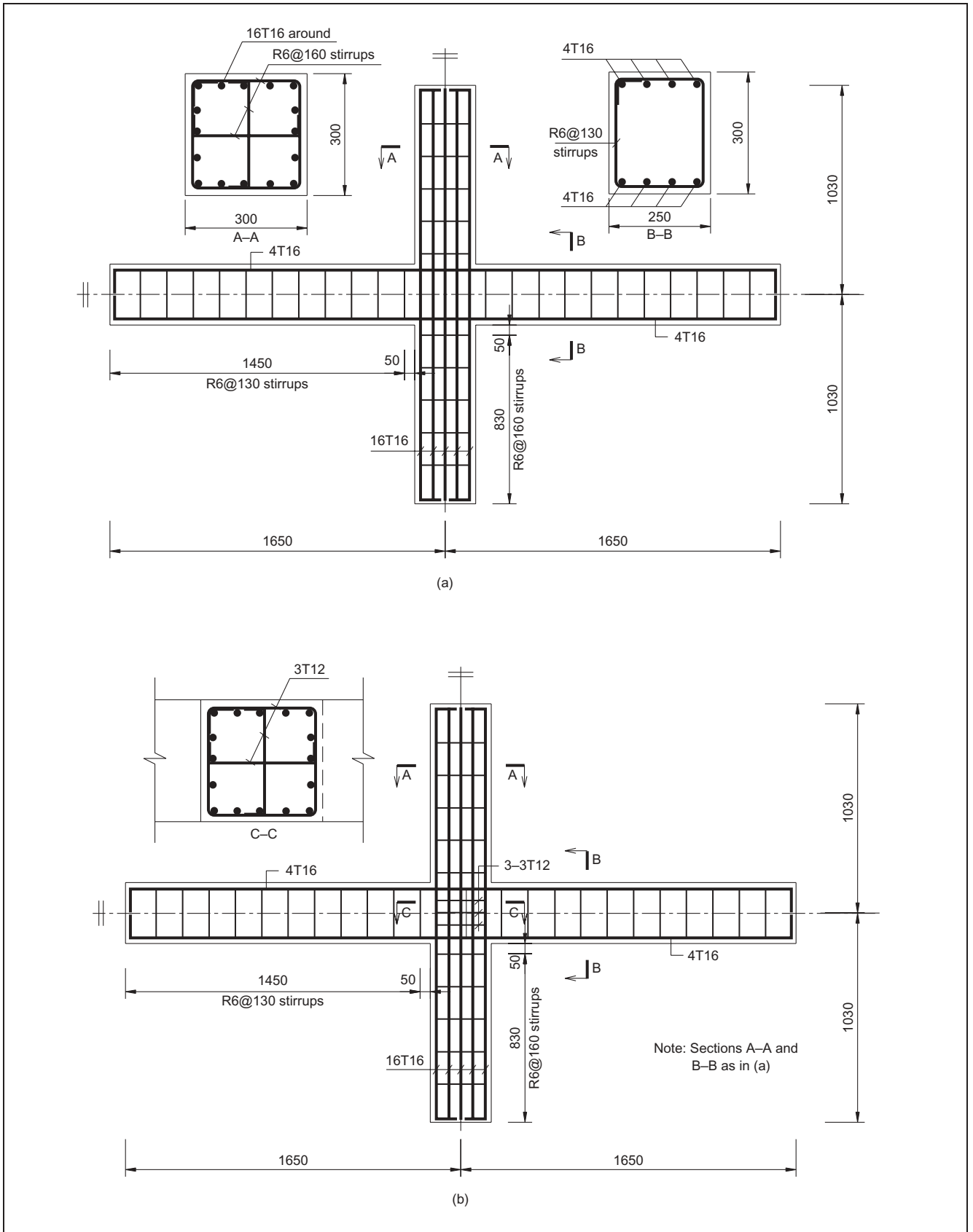

Fig. 4. Reinforcement details of beam–column joint specimens: (a) series E; (b) series H (dimensions in mm)

strut mechanism should not exceed the bearing capacity of concrete, and the following rule (clause 2·10·1·3(6)) is specified.

3	$V_{\text{jhd}} \leq 20\tau_{\text{Rd}} b_{\text{j}} h_{\text{c}}$

where τ_{Rd} = basic design shear strength of member without shear reinforcement (0·35 N/mm^2); b_{j} = effective joint width (300 mm); and h_{c} = width of column in the direction of beam (300 mm).

In the present case, the shear force acting on the concrete core

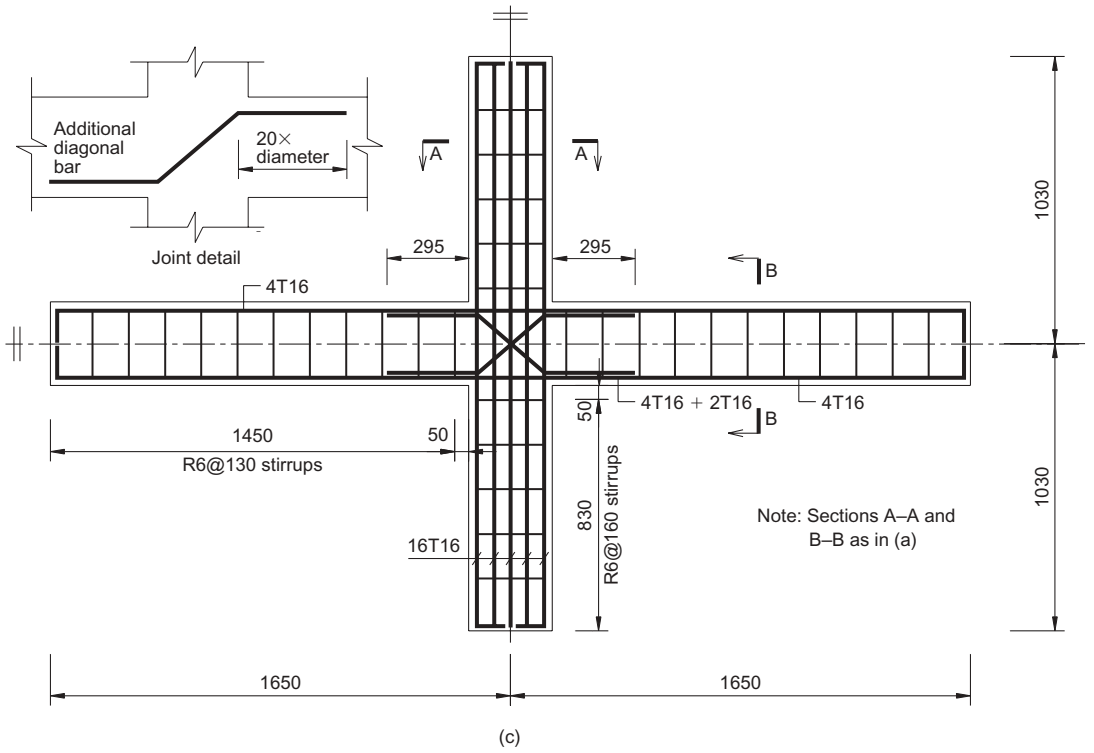

Fig. 4. (Continued) (c) Series AD (dimensions in mm)

of the joint V_{jhd} is estimated using equation (2) as 419·7 kN and it is well below the limit of 630 kN evaluated by equation (3). The transverse reinforcement required A_{sh} is given by (clause 2.10.1.3(8))

$$\frac{A_{sh} f_{yd}}{b_j h_{jw}} = \frac{V_{jhd}}{b_j h_{jc}} - \lambda \sqrt{\tau_{Rd}(12\tau_{Rd} + \upsilon_d f_{cd})} \quad (4)$$

where h_{jw} = distance between top and bottom reinforcement in beam (242 mm); h_{jc} = distance between reinforcement at two faces in column (242 mm); λ = factor accounting for the available shear resistance of plain concrete after cyclic degradation (1·2 for DC 'M'); υ_d = normalised design axial force (0·0); and f_{cd} = design value of concrete compressive cylinder strength ($\cong 0{\cdot}8\, f_{cu} = 32$ MPa).

As the absence of axial load in the column is more critical than if it is loaded, the required transverse reinforcement A_{sh} is calculated assuming no axial load, and it turns out to be 683 mm^2. Therefore the provided transverse reinforcement of 1018 mm^2 is adequate according to Eurocode 8.[14]

Each joint of the AD-series is provided with additional diagonal steel bars in two opposite directions, as shown in Fig. 4(c). From the preliminary findings,[10] the concrete in the joint containing diagonal bars is capable of resisting a fair proportion of the horizontal joint shear force, and therefore the equivalent reinforcement area required for the diagonal bars is taken to be 70% of that of the normal transverse reinforcement, namely

$$2A_{sd} \cos\theta = 0{\cdot}7 A_{sh} \quad (5)$$

where A_{sd} = total area of diagonal steel bars in one direction; and θ = inclination of diagonal bars (45° in the present case).

With the value of A_{sh} of 683 mm^2 worked out according to Eurocode 8,[14] the total area of diagonal steel bars in one direction, A_{sd}, can be calculated as 338 mm^2. Therefore 2T16 diagonal bars (402 mm^2) of zigzag shape are provided in each direction. Each bar has horizontal tails projecting into the adjacent beams so that a development length of 20 diameters of the bar is provided as measured from the centre of the nearest bend (Fig. 4(c)).

Table 1 summarises the properties of specimens tested together with the material strengths. For each specimen, three steel bars were tested in tension. The actual yield strengths of steel were usually well above the specified value of 460 MPa for high-yield steel. Six concrete cubes were made when each specimen was cast, and they were exposed to a similar environment as the specimen. Three were tested 28 days after casting while the others were tested at the time of testing to determine the theoretical strength of the specimen. The original design concrete cube strength was 40 MPa at 28 days. However since the actual tests were very often performed beyond that date, further increase in concrete strength was also noted. It is noted that in the estimation of joint reinforcement for all the specimens, the design yield strength of steel has been used. If the actual yield strength is adopted, the required joint reinforcement will be increased, but the reinforcement provided is still sufficient. In addition, the volumetric ratios of steel

Unit	Axial load level: $P/f_{cu}A_g$	Yield strength of longitudinal bars f_y: MPa	Concrete cube strength f_{cu}: MPa	Joint detailing	
				Pattern	ρ_h: %
E-0·0	0·0	513·3	43·1	Empty	N/A
H-0·0	0·0	594·7	50·6	Hoops 3-3T12	1·40
AD-0·0	0·0	558·4	42·6	Diagonal bars 2-2T16	1·36
E-0·3	0·3	558·4	46·1	Empty	N/A
H-0·3	0·3	518·0	45·1	Hoops 3-3T12	1·40
AD-0·3	0·3	538·2	39·4	Diagonal bars 2-2T16	1·36

Table 1. Summary of specimens tested

relative to the core concrete ρ_h are also shown. This volumetric ratio is calculated based on the rectangular reference volume defined by the dimensions h_{jc}, h_{jw} and b_j as defined before.

3.2. Test setup, instrumentation and loading procedure

Each of the specimens was tested in a self-reacting steel frame as shown schematically in Fig. 5. The column was held in place by the top and bottom hinges to simulate the inflection points of the column. In addition, the bottom hinge was vertically movable so that axial load could be applied using a jack (jack 3) below the column if required. Reversed cyclic quasi-static loads to simulate earthquake forces were applied via a pair of 500 kN MTS servo-controlled hydraulic actuators (jacks 1 and 2) at the ends of the beam in an anti-symmetric manner. During the tests, jacks 1 and 2 were largely acting in opposite sense with approximately the same magnitude. This couple was resisted by another couple of equal and opposite horizontal reactions at the top and bottom hinges, which were actually the column shear force V_c given by

$$V_c = \frac{P_1 - P_2}{2} \times \frac{L_b}{L_c} \quad (6)$$

where P_1 and P_2 = forces applied by jacks 1 and 2 respectively (upward as positive); L_b = distance between jacks 1 and 2 (3000 mm); and L_c = distance between top and bottom hinges for the column (2665 mm).

Figure 6 shows the instrumentation provided to monitor the deformation and strains at various locations. Two linear variable displacement transducers (LVDTs) were mounted at the beam ends to monitor deflections so that the relationship between storey shear and storey drift could be worked out with

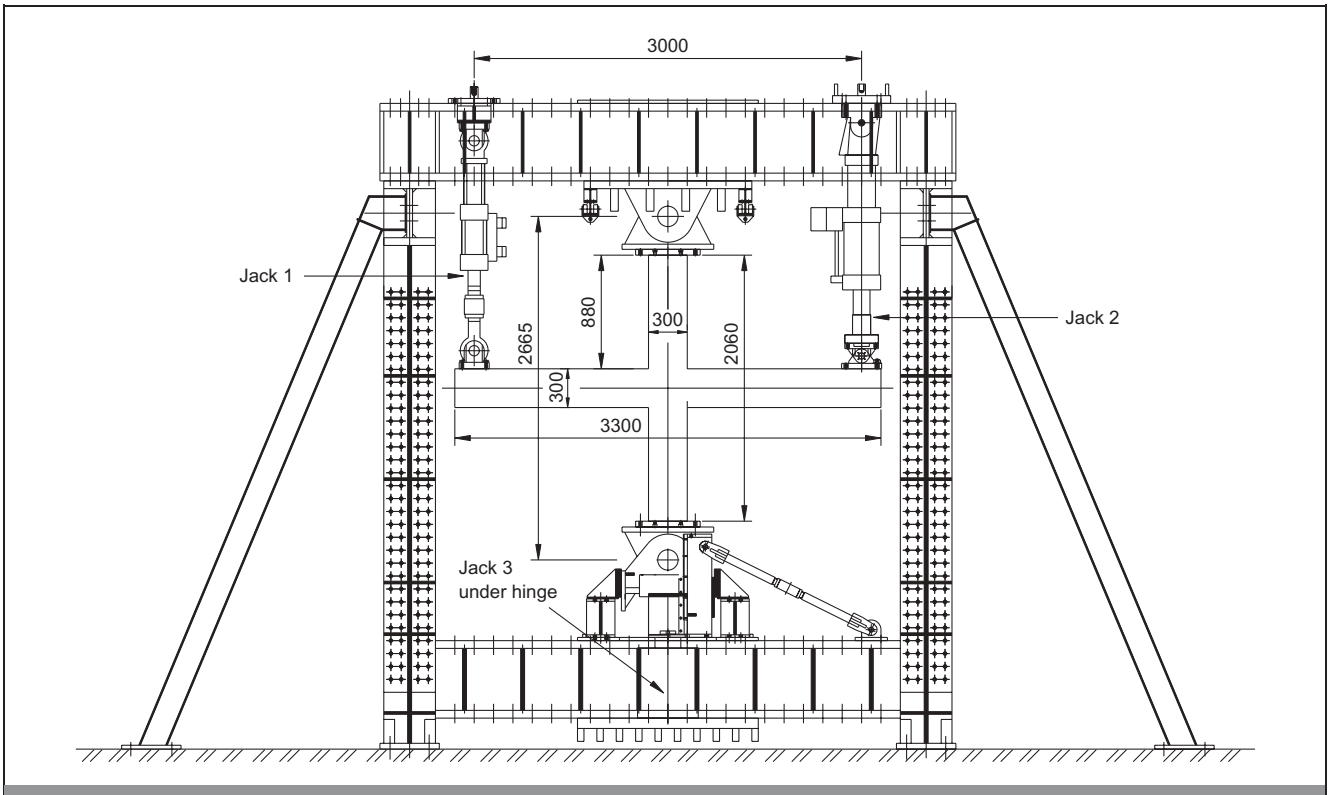

Fig. 5. Set-up for testing of beam–column joint specimens (dimensions in mm)

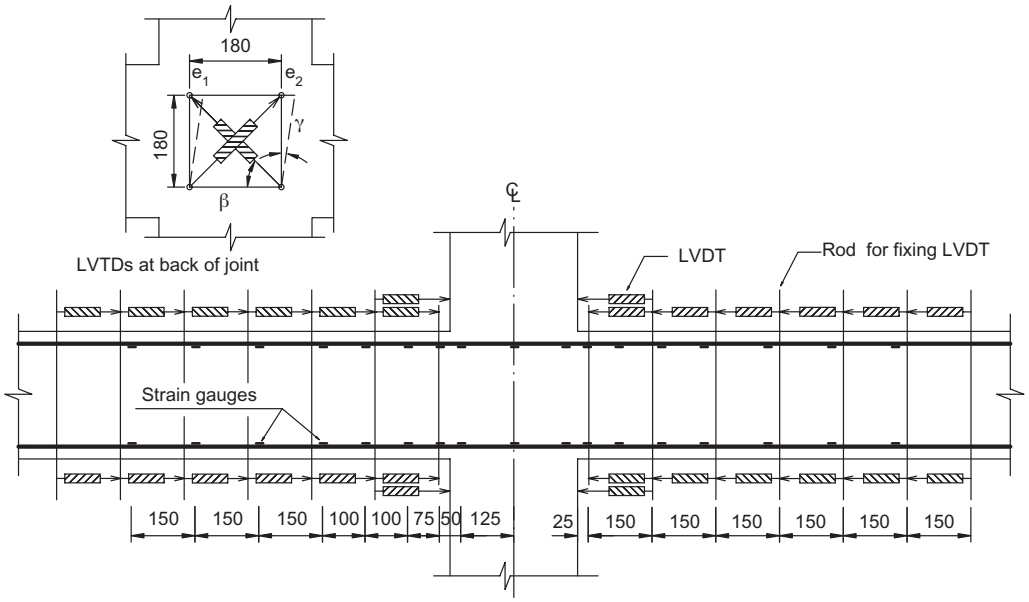

Fig. 6. Major instrumentation along beam (dimensions in mm)

reference to Fig. 1(b). The equivalent column drift Δ_c and the drift ratio η can be written as

$$\Delta_c = \frac{\Delta_1 - \Delta_2}{L_b} \times L_c \quad (7a)$$

$$\eta = \frac{\Delta_c}{L_c} - 100\% \quad (7b)$$

where Δ_1 and Δ_2 are the beam displacements at jacks 1 and 2 respectively (upward as positive). For estimation of the average beam curvatures, LVDTs were also mounted in pairs both above and below the beam. The two pairs of LVDTs adjacent to each column face enabled the estimation of crack width at the beam–column interface. In addition, two LVDTs were positioned diagonally on the rear face of the joint to detect the shear distortion. Electrical resistance strain gauges were used to monitor strain variation along selected reinforcing bars. All strain gauges were stuck along the centreline of the reinforcing bar such that the local bending effect could be eliminated. All the LVDTs and strain gauges were connected to a logger for data acquisition.

3.3. Loading procedure

The nominal flexural strength M_n of the beam in each specimen was first evaluated based on the material properties at the time of testing using BS 8110[6] taking all partial factors of safety as unity. After applying the column axial load if required, the simulated seismic loading was then applied under load-control mode in the first cycle and displacement-control mode in the subsequent cycles of the specimen. A full loading cycle consisted of a half cycle in the positive direction, in which jacks 1 and 2 acted in tension and compression respectively, followed by another half cycle in which jacks 1 and 2 worked in the opposite sense. The peak load in the first cycle was chosen so that the maximum bending moment of the beam reached 75% of its nominal flexural strength M_n. In this cycle, the peak displacements measured at the beam ends both in the positive and negative half cycles were recorded. The absolute values of these four measurements were then averaged and denoted as $0{\cdot}75\Delta_y$, from which the nominal yield displacement Δ_y can be easily calculated. In the second cycle, the beam ends were incrementally displaced to $+\Delta_y$ in the positive direction within the positive half cycle and then $-\Delta_y$ (in the opposite direction) within the negative half cycle. The displacement ductility factor μ is defined as the ratio of peak displacement Δ to the nominal yield displacement Δ_y. The specimen was therefore considered to have reached displacement ductility factor μ equal to +1 and −1 in this cycle. Starting with displacement ductility factor $\mu = 2$, two loading cycles of the same displacement ductility factor μ were carried out before increasing μ by one until the load-carrying capacity of the specimen fell below 80% of its maximum measured strength. The loading sequence is summarised in Fig. 7. The loading or displacement was applied by convenient

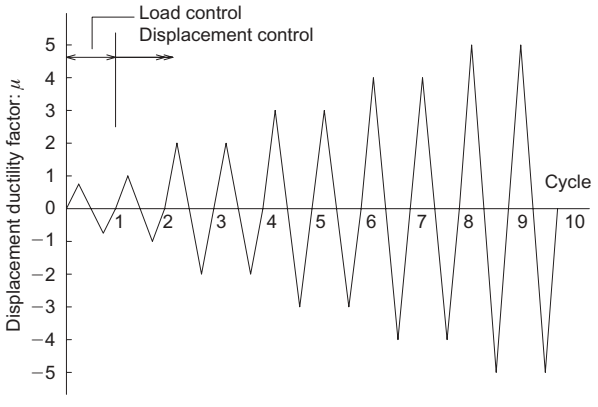

Fig. 7. Loading sequence

increments to facilitate data recording. At the peak of each half cycle, cracks were marked on the specimen and photographs were taken.

4. EXPERIMENTAL RESULTS AND DISCUSSION

4.1. General observations

All the specimens developed diagonal cracks on the surface of the joint on reaching the first half loading cycle—that is, causing 75% of the nominal flexural strength M_n of the beam. Most of the crack patterns were common to one another. The cracking became more serious with further loading cycles leading to concrete spalling at various locations. Because of the coexisting bending moments and shear forces in the beam and column, flexural and shear cracks of different severity were also progressively formed. The cracking patterns of the specimens with axial loading in the column were largely similar to those without column axial load. However the presence of the axial loading in the column helped to reduce the cracking in the column and damage to the joint. The vertical compressive stresses in the joint also increased the inclination of the diagonal cracks in the joint.

Unit E-0·0 was characterised by relatively more serious damage to the joint in the form of cracking and spalling, as compared to the adjacent parts of beam and column. The failure of the specimen was preceded by crushing of the joint concrete and dramatic loss of stiffness. Similar severe damage to the joint was observed in unit H-0·0 together with serious cracks in the beam adjacent to the column face—that is, the beam–column interface cracks, at the beam. The behaviour of unit AD-0·0 at the early stage of testing was similar to that of unit H-0·0, but further damage in the form of spalling did not happen until the displacement ductility factor reached $\mu = 3$. It should be noted that throughout the test, the beam–column interface crack was insignificant in unit AD-0·0 because of the existence of the diagonal bars. The damage of units E-0·0, H-0·0 and AD-0·0 at displacement ductility factor $\mu = 3$ is shown in Fig. 8.

There were certain similarities in the behaviour of the beams in different series. Flexural cracking first appeared followed by inclined shear cracks at a later stage. However, unit AD-0·0 displayed rather complicated cracking patterns including flexure, shear and splitting. The development lengths of the diagonal bars within the beam did enhance the strength to a certain extent and limited the beam–column interface crack at the column face. In the vicinity of the ends of the diagonal bars, more severe damage of the beam was observed. Inclined cracks developed through the beam section to the other side causing spalling of the concrete, indicating critical shear action. In addition, some nearly horizontal cracks along the development length of the diagonal bars were observed suggesting bond deterioration. A summary of the experimental observations for each specimen is presented in Table 2. It shows the nominal flexural strength M_n of the beams, the applied loads at which cracking occurred, the maximum joint shear forces observed, and the failure modes and damage observed. The apparent variation of the nominal flexural strength M_n of the beams was caused by the natural variation of material strengths. The presence of axial loading generally raises the cracking load but this effect is insignificant for the H-series. In particular, the maximum joint shear force V_{jh} for

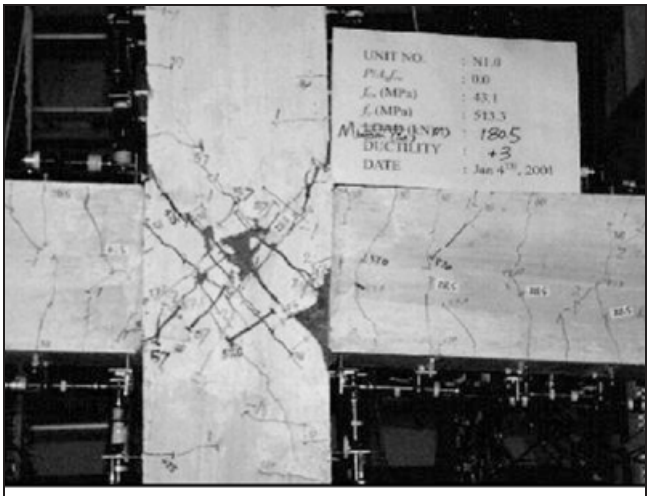

(a)

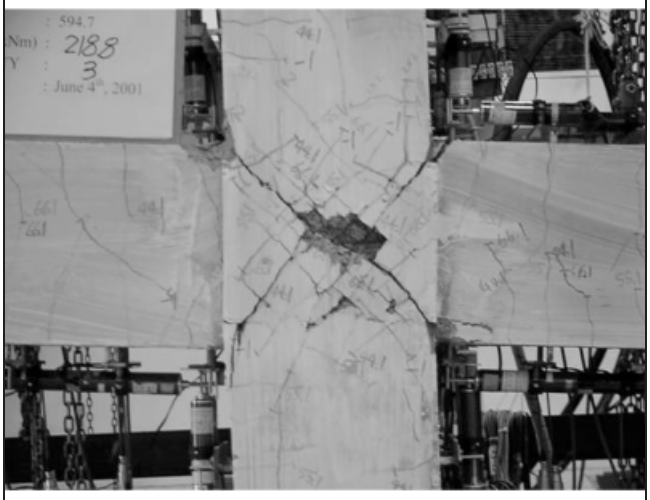

(b)

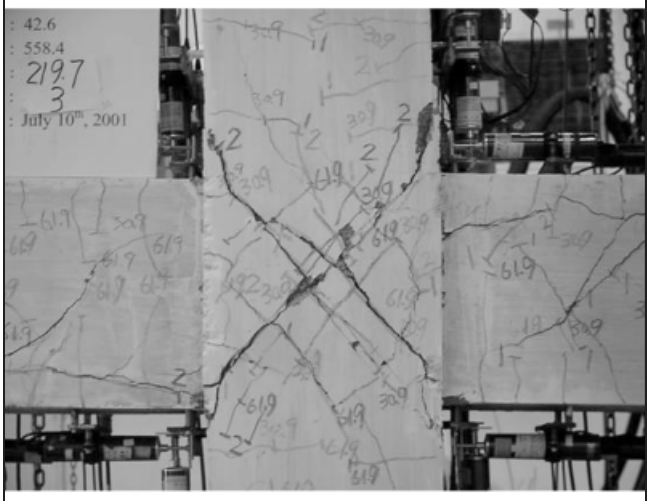

(c)

Fig. 8. Observed damage to joints with zero axial load: (a) unit E-0·0; (b) unit H-0·0; (c) unit AD-0·0

each case was calculated based on equation (1) using the applied loading, the tension carried by the beam reinforcement inferred from strain gauge readings, and the fact that the compression was equal in magnitude to the tension at a beam section. The joint shear strengths of the AD-series are much higher than the others, indicating the contributions from the additional diagonal bars. It was observed that all specimens eventually failed by shear at the joint with different degrees of

Unit	Beam nominal flexural strength M_n: kNm	Cracking load: kN	Max. joint shear V_{jh}: kN	Failure mode	Damage observed
E-0·0	102·6	38·0	750·4	Joint shear failure	Beam intact, bending capacity not yet reached
H-0·0	119·0	55·1	869·3	Joint shear failure	Beam almost intact, bending capacity not yet reached
AD-0·0	111·4	30·9	1175·5	Joint shear failure	Beam slightly damaged, bending capacity reached
E-0·3	111·7	62·1	813·9	Joint shear failure	Beam intact, bending capacity not yet reached
H-0·3	103·8	57·7	743·9	Joint shear failure	Beam almost intact, bending capacity not yet reached
AD-0·3	107·2	59·6	1049·2	Joint shear failure	Beam slightly damaged, bending capacity reached

Table 2. Summary of experimental observations

damage to the beam. The beams in units E-0·0, E-0·3 and H-0·0 did not develop fully their bending capacities. On the other hand, those of the AD-series reached their bending capacities with plastic hinges formed in the beams at a distance from the column faces, which is desirable for earthquake-resistant structures. To sum up, the AD-series takes the highest load.

4.2. Hysteretic response of column shear force versus storey drift

The equivalent storey drift Δ_c and the drift ratio η are plotted against the column shear force V_c for each of the specimens, and the results are shown in Fig. 9. The nominal shear strength V_n of the column calculated based on the corresponding nominal flexural strength M_n of the beam for each specimen is also shown for comparison. Also plotted on the graphs for convenience are the ductility factors μ. The ratio of the measured equivalent column shear strength V_{max} to the nominal shear strength V_n for each specimen is also listed in Table 3. This ratio is also identical to that of the measured maximum bending moment in the beam to the corresponding nominal value. The hysteretic loops shown in Fig. 9 are useful for assessment of the degradation of load-carrying capacity. All of them show pinching to different extents at ductility factors μ greater than two. The envelopes of the hysteretic curves of column shear force versus displacement ductility factor for all the specimens are plotted in Fig. 10. The ultimate ductility factor μ_u and the ultimate drift ratio η_u at failure are determined from interpolation using the positive cycles of these envelopes. It is assumed that failure occurs when the column shear force V_c drops to 80% of V_{max} after reaching the peak. From the values of μ_u and η_u listed in Table 3, the specimens without column axial loading can be arranged from the least to the most ductile in the following order: unit E-0·0 with $\mu_u = 2{\cdot}9$ and $\eta_u = 3{\cdot}1$, unit AD-0·0 with $\mu_u = 3{\cdot}2$ and $\eta_u = 3{\cdot}0$, and unit H-0·0 with $\mu_u = 3{\cdot}9$ and $\eta_u = 5{\cdot}0$. In the presence of an axial load level $P/f_{cu}A_g$ of 0·3 in the column, improvement in the ultimate ductility factor μ_u is noted, but the same sequence of ductility is still observed. The ultimate drift ratios η_u also decrease.

Judging from Figs 9 and 10, units in the E-series had the least strength and their strength sustainability is also inferior to those of the other series. After reaching the peak resistance, the strength dropped fairly rapidly in subsequent cycles. For example, units E-0·0 and E-0·3 had losses of strength amounting to 20% and 14% respectively in the following two cycles after reaching the peak. Both units E-0·0 and H-0·0 could not reach the nominal strengths because of premature failure at the joint. It is interesting to note that although the hoop reinforcement in unit H-0·0 did not enhance the strength, it did improve its strength sustainability beyond the peak. In contrast, unit AD-0·0 achieved the nominal strength with slight enhancement, which appeared to be related to the development length of the diagonal bars. It should also be noted that the development length provided in the beam was only 20 times the bar size, which was far less than the full tension anchorage length of 35 times the bar size as recommended by BS 8110.[6] In addition, the contribution from the diagonal bars was ignored in the calculation of nominal flexural strength of the beam.

The presence of column axial load did enhance the strengths of all units to various degrees as summarised in Table 3. For the E-series, the column axial load had very little effect on the peak strength and strength sustainability beyond the peak. For the H-series, the column axial load not only improved the peak strength but also enhanced the strength sustainability beyond the peak. For example, in the presence of column axial load, the strength of unit H-0·3 remained fairly close to the peak strength even up to a ductility factor μ of 4. Similar beneficial effects of the column axial load are observed in the AD-series with diagonal bars. In the presence of column axial load, the strength increased from 103 to 110% of the nominal strength. Up to a ductility factor μ of 2, the strength behaviour of various specimens was not very much affected by the column axial load. Unit AD-0·0 showed a drop in strength beyond $\mu = 2$, but the strength reduction was only observed in unit AD-0·3 beyond $\mu = 3$. Therefore the units with diagonal reinforcement are fairly reliable for low to medium seismicity in which the demand for ductility is not as great. The H-series generally displayed better strength sustainability at high ductility factors, and that explains why hoops are commonly used in cases of high seismicity.

4.3. Stiffness degradation

With the damage accumulated in cycles of load reversals, all specimens suffered from stiffness degradation for various reasons. The formation of additional flexural and shear cracks

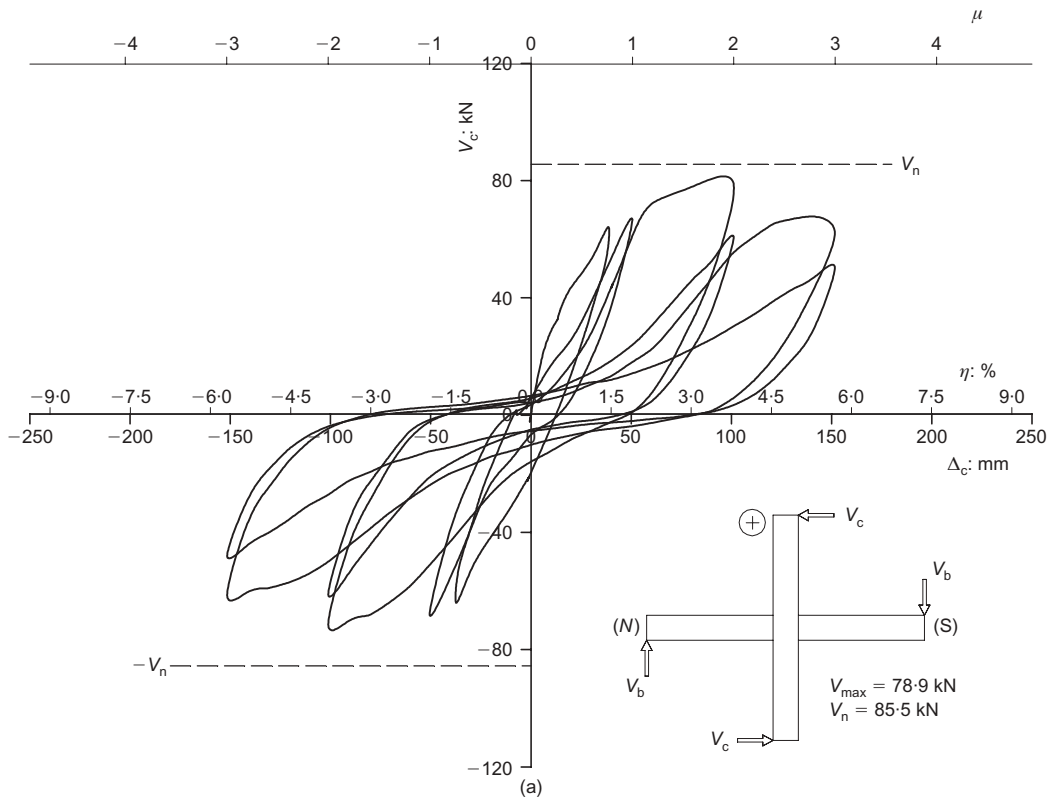

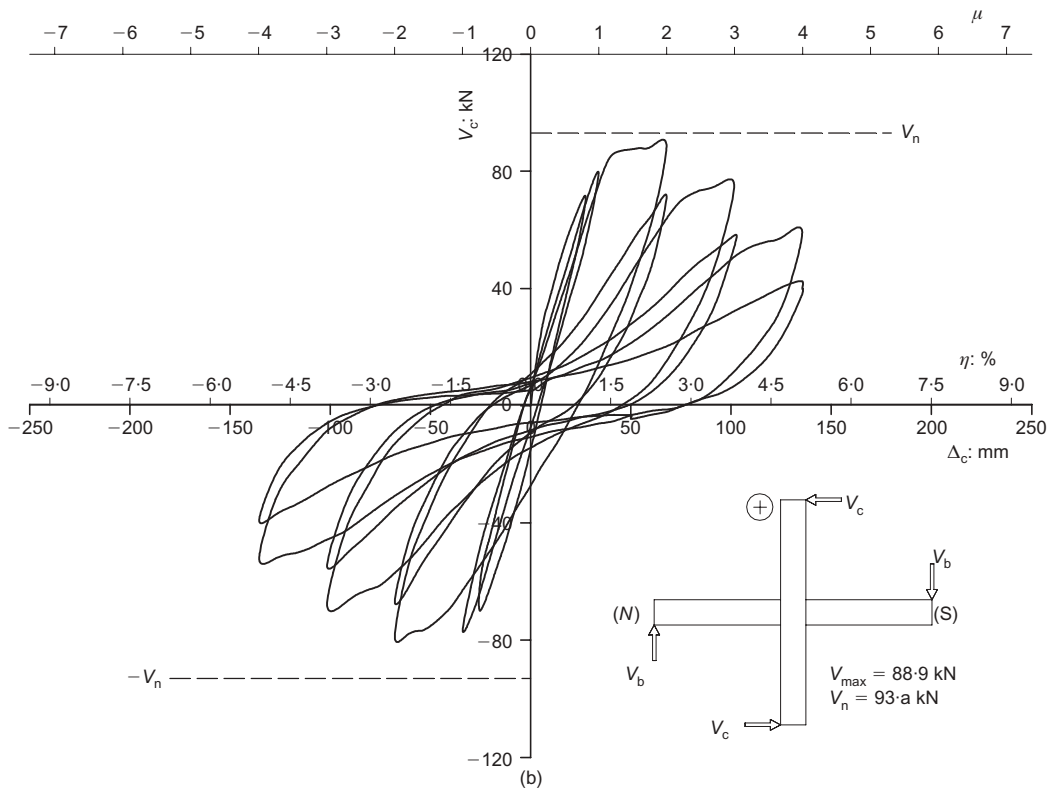

Fig. 9. Hysteretic loops of column shear force V_c against storey drift Δ_c: (a) unit E-0·0; (b) unit E-0·3

weakened the structure. The residual strains of reinforcement accumulated over the load cycles not only made difficult the closing of a crack after opening, but also caused bond slip in the vicinity. All these features led to reductions in both the axial and flexural stiffnesses as well as their corresponding resistances. Therefore the hysteretic loops display pinching to different extent at ductility factors μ greater than two.

The slope of the straight line joining a peak of each hysteretic loop of column shear force against storey drift to the origin is the secant stiffness for that half cycle. The average stiffness obtained for the two half cycles in a hysteretic loop therefore gives the representative stiffness for that particular cycle. Fig. 11 shows the average secant stiffnesses for the first of the cycles for each ductility factor, expressed as a percentage of

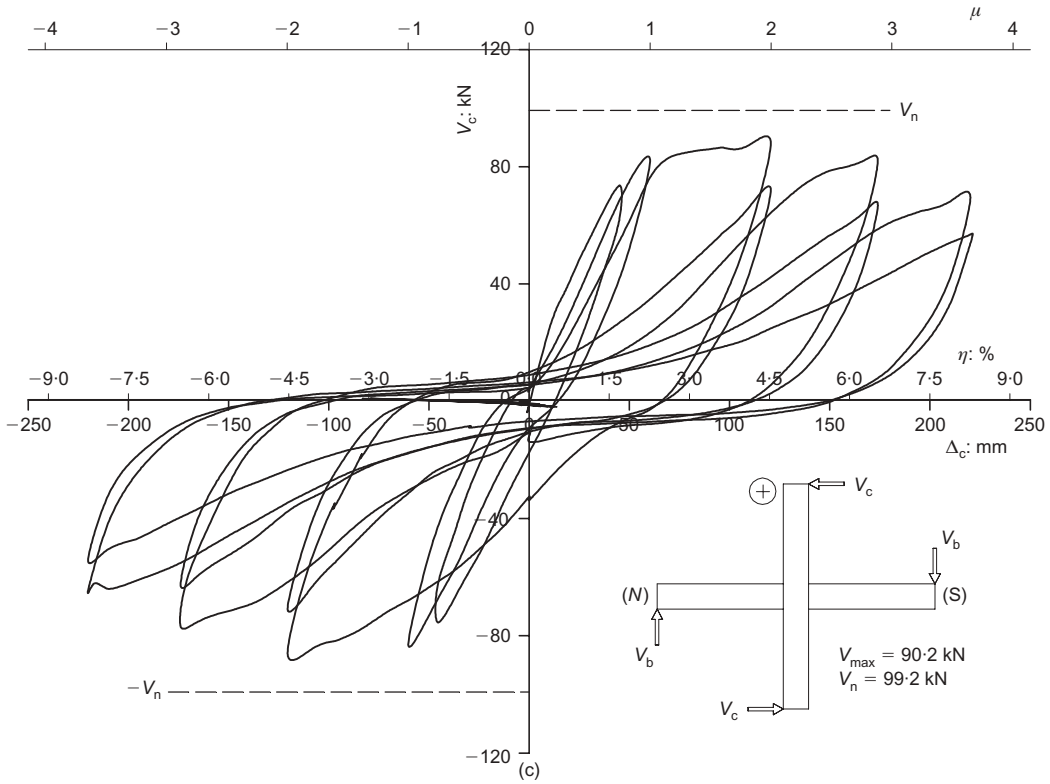

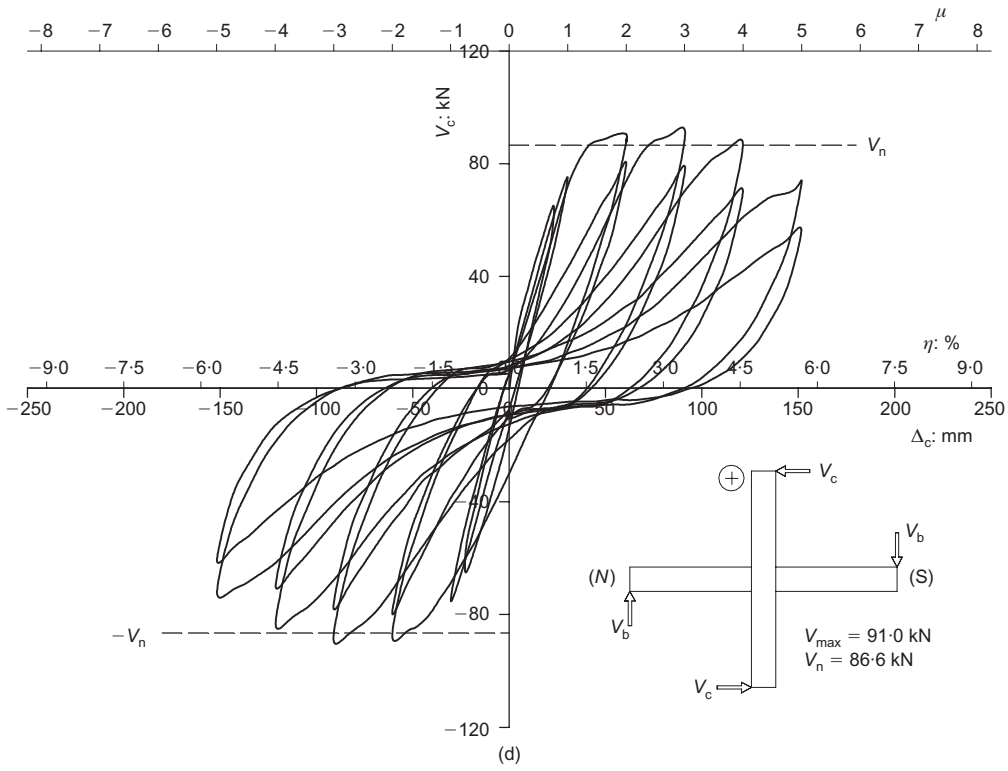

Fig. 9. (Continued) (c) unit H-0·0; (d) unit H-0·3

the initial elastic stiffness obtained in the first cycle. All specimens suffered from stiffness degradation amounting to around 50% at a ductility factor μ of 2. Units of the AD-series with the diagonal bars degraded less rapidly in stiffness up to a ductility factor μ of 3 compared with the others, although the H-series performed slightly better beyond $\mu = 3$. The stiffness degradation of the E-series was the worst of all. In all three series, the presence of column axial load was beneficial to the preservation of stiffness. According to the loading procedure specified, a repeated cycle was carried out at ductility factors μ of 2 and above. All specimens suffered from further stiffness degradation in the repeated cycle. This was the most acute in

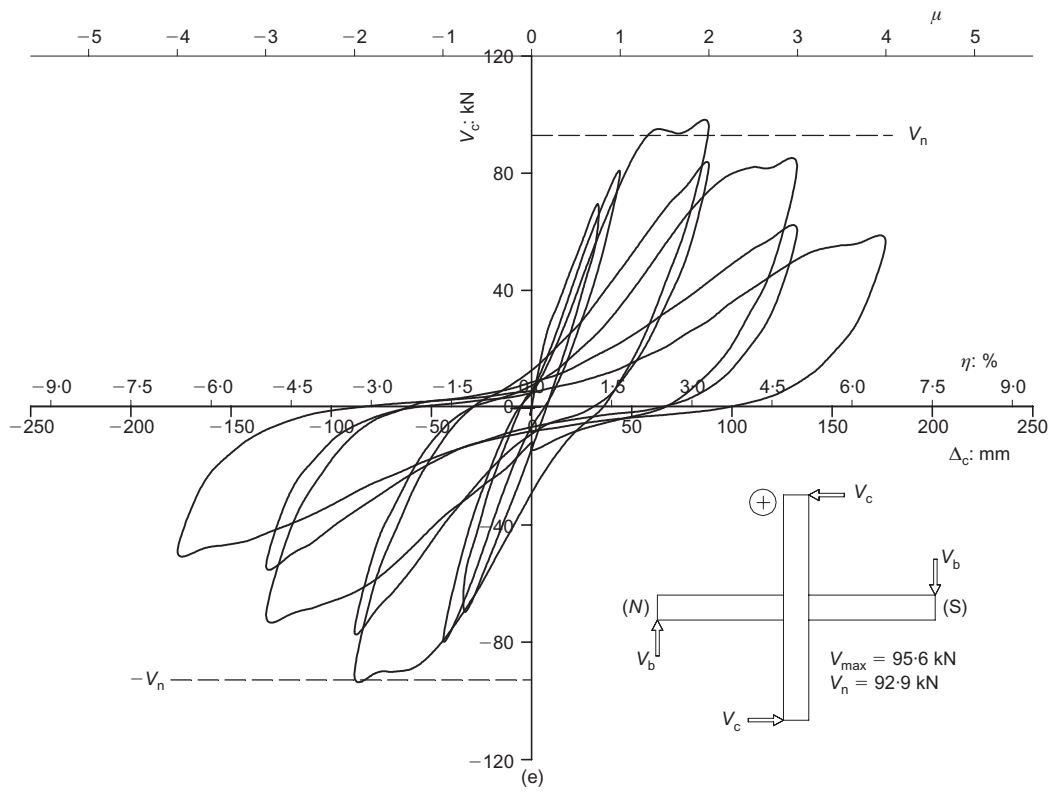

Fig. 9. (Continued) (e) unit AD-0·0; (f) unit AD-0·3

the E-series. Units of the AD-series performed fairly well up to a ductility factor μ of 2, but they deteriorated beyond it. Comparatively speaking, further stiffness degradation in the repeated cycle was reasonably low for units of the H-series up to ductility factors μ of 4.

4.4. Joint distortion

The stress conditions in the beam–column joint are indeed rather complicated. The interior core of the joint bounded by the longitudinal bars in the beam and column is in fact subject to larger shear stresses and therefore will have more distortion

Unit	Max. column shear strength V_{max}/nominal column shear strength V_n	Ultimate ductility factor: μ_u	Ultimate column drift ratio η_u: %
E-0·0	0·92	2·9	3·1
H-0·0	0·89	3·9	5·0
AD-0·0	1·03	3·2	3·0
E-0·3	0·96	3·2	2·3
H-0·3	1·05	5·0	3·2
AD-0·3	1·10	4·0	2·5

Table 3. Summary of ultimate results

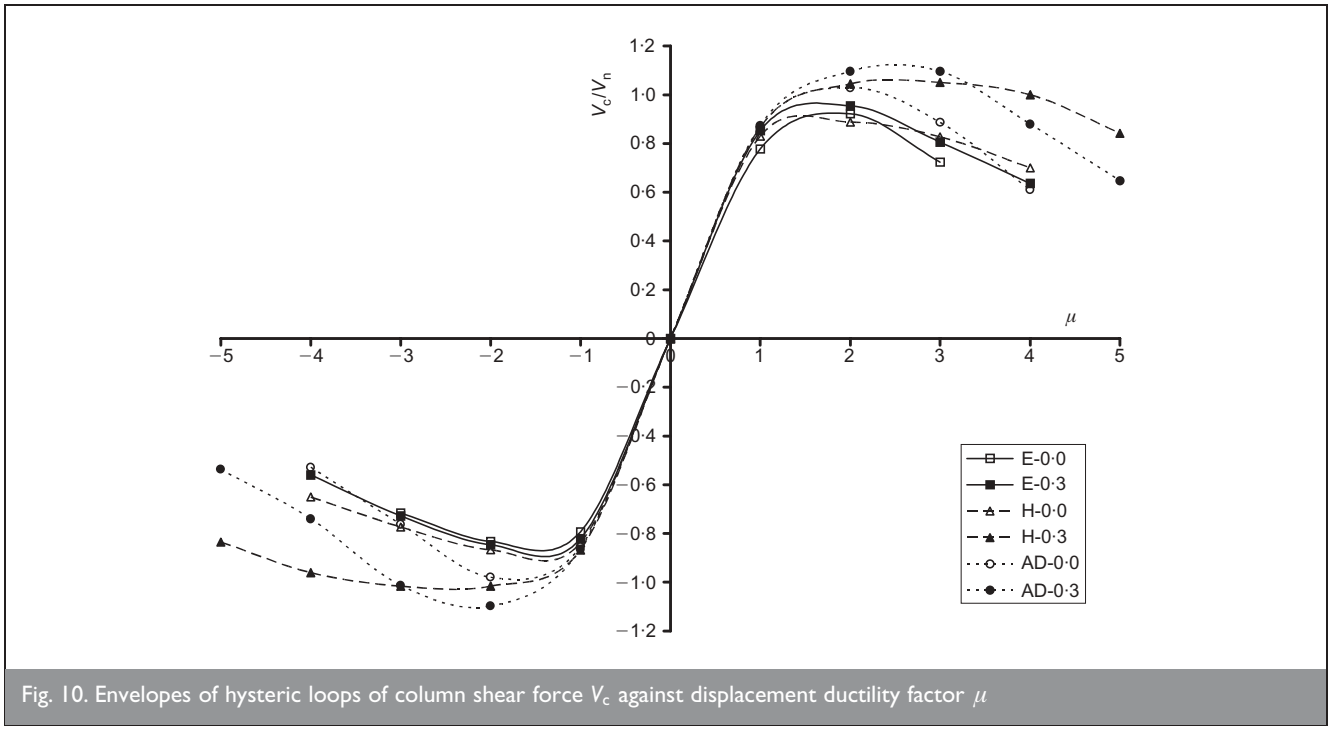

Fig. 10. Envelopes of hysteric loops of column shear force V_c against displacement ductility factor μ

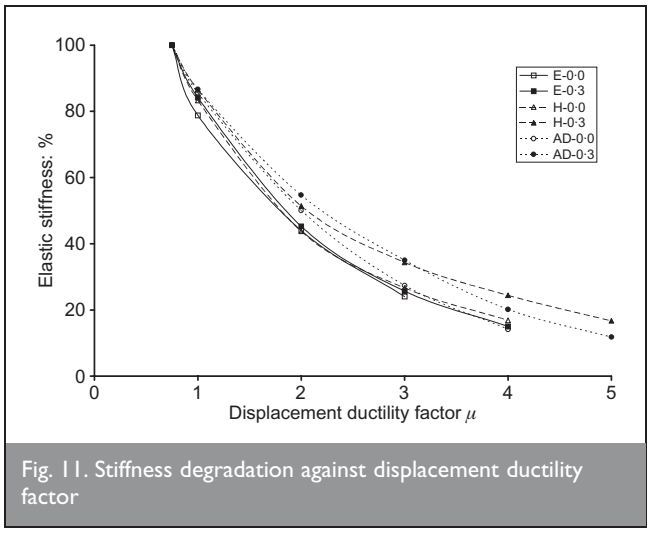

Fig. 11. Stiffness degradation against displacement ductility factor

compared with the entire joint. The two LVDTs mounted diagonally on the rear face of the joint as shown in Fig. 6 were essentially to detect the shear distortion of the interior core of the joint. The joint distortion γ can be estimated as

$$\gamma = \frac{e_1 - e_2}{2 l_j}(\tan\beta + \cot\beta) \quad (8)$$

where e_1 and e_2 = readings of LVDTs (extension as positive); l_i = initial distance between mounting rods; and β = initial inclination of LVDTs to horizontal.

The use of such measured shear strain without suitable correction in the evaluation of its contribution to storey drift may lead to overestimation. Nevertheless, examination of the joint distortion still provides another aspect by which to judge the performance of different joint detailing. For the first of the cycles for each ductility factor, the absolute values of maximum joint distortion in the two half-cycles are averaged and plotted against the ductility factor μ in Fig. 12.

The LVDTs were mounted on rods embedded in concrete. The accuracy of measurements therefore relied upon these rods remaining normal to the plane of the specimen throughout the test. After a large number of cycles have been imposed on a

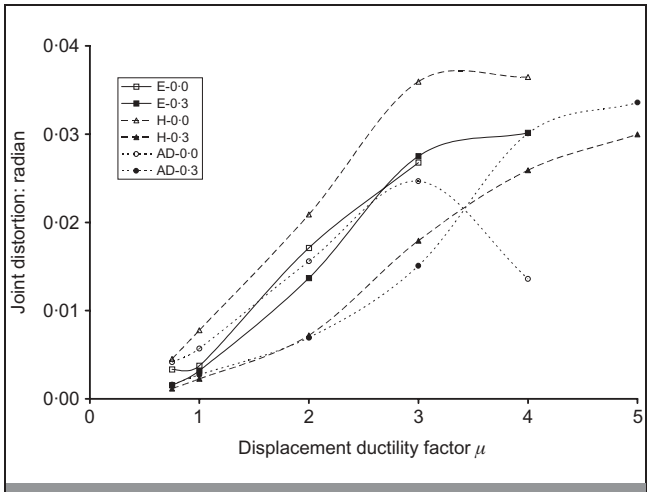

Fig. 12. Joint distortion against displacement ductility factor

specimen, the rods for mounting LVDTs might no longer be normal to the plane of the specimen because of spalling of concrete cover and other reasons. Therefore the accuracy of the measurements at large ductility factors may not be as reliable. The joint distortion is affected not only by the imposed displacements at the beam ends and the distribution of deformation within the specimen, but also by the actual strength of the unit at the stage. It is observed that the column axial load was beneficial to the control of joint distortion for the H- and AD-series, but not the E-series. The presence of the diagonal bars in the units of the AD-series was rather effective in controlling the diagonal tensile cracking in the joint. In general, the joint distortion of the AD-series was relatively low compared with the others, while that of the E-series was relatively high. In comparison, the column axial load governed the performance of joint distortion of the H-series. In the absence of column axial load, the joint distortion of unit H-0·0 had been the maximum of all. On the contrary, unit H-0·3 had joint distortion much reduced approaching that of AD-0·3. The stress conditions of the confined joint core of the H-series under column axial load were considered helpful in controlling joint distortion. The significant reduction in joint distortion of unit AD-0·0 for ductility factor μ above 3 was likely to be caused by measurement errors, although the joint distortion was expected to drop slightly in view of the reduction of strength as shown in Fig. 10.

It was also noted that the rates of displacement in the tensile and compressive diagonals were different. Displacement along the tensile diagonal was often much quicker than that in the compressive diagonal. With the reversal of loading, the extensions in the previous cycles were often not fully recovered therefore resulting in gradual dilation of the joint.

4.5. Crack at beam–column interface

The beam–column interface cracks were often the most noticeable cracks formed during the tests. With the progress of the test, these cracks developed rapidly not only in width but also in depth. After several cycles of load reversals and the accumulation of plastic deformation in the reinforcing bars, the compression zone in the concrete gradually shrank, leading to crushing and spalling at certain locations. The beam–column interface cracks of certain specimens also developed into the joint core creating further deterioration there. Earlier research [15] revealed that the beam–column interface crack could create significant deflection at the beam end amounting to as much as 50% of the total. This is also a major reason for the stiffness degradation. As far as the beam in a specimen was concerned, the beam–column interface cracks caused fairly concentrated curvature there, resulting in significant deflection at the beam end. As explained before, the two pairs of LVDTs adjacent to each column face were provided to pick up such effects. The percentage of the total deflection at a beam end caused by the beam–column interface cracks was estimated for the first cycle at each value of ductility factor and plotted in Fig. 13. The need for such instrumentation was only realised after testing unit E-0·0.

From the available data, it was observed that beam–column interface cracks became more significant with further load reversals. The column axial load also had a marginal beneficial effect on the control of beam–column interface cracks. Up to a ductility factor μ of 1, performance of all specimens in respect of interface cracking were fairly similar. However at ductility factor μ of 2 and above, the effects of interface cracking were much more serious in the E- and H-series. Comparatively specimens in the AD-series had much better control of interface cracking. It can therefore be concluded that the diagonal bars are much more effective in controlling beam–column interface cracks than nominal hoops inside the joint.

4.6. Curvature profile along beam

The average beam curvatures were estimated using readings from LVDTs mounted in pairs above and below it. The curvature profiles of units E-0·3, H-0·3 and AD-0·3 at various ductility factors are plotted in Fig. 14. The location of maximum curvature normally suggests the formation of plastic hinge there. The formation of plastic hinges at suitable locations of a structure is often beneficial to the overall stability during an earthquake. However, because of the large amount of deformation involved, a lot of damage is also expected. The locations where plastic hinges may form in an earthquake will therefore govern the repairability of a structure. Figure 14 shows that for units E-0·3 and H-0·3, the maximum curvatures occur at the column face. The abrupt increase of the curvature near the column face at high ductility factors resulted in significant bond-slip effect at the beam–

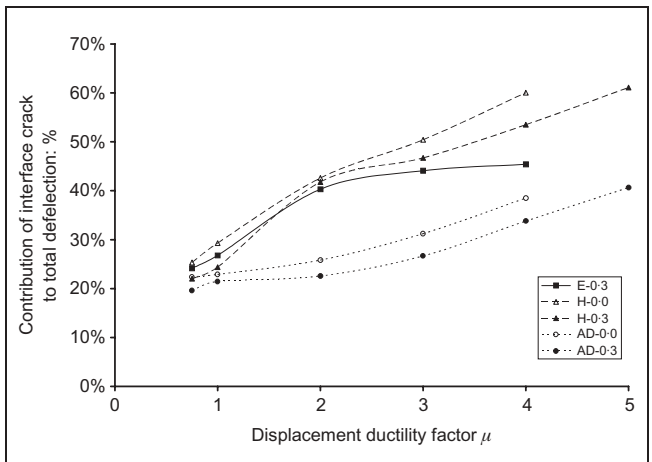

Fig. 13. Contribution of beam–column interface crack to total beam deflection

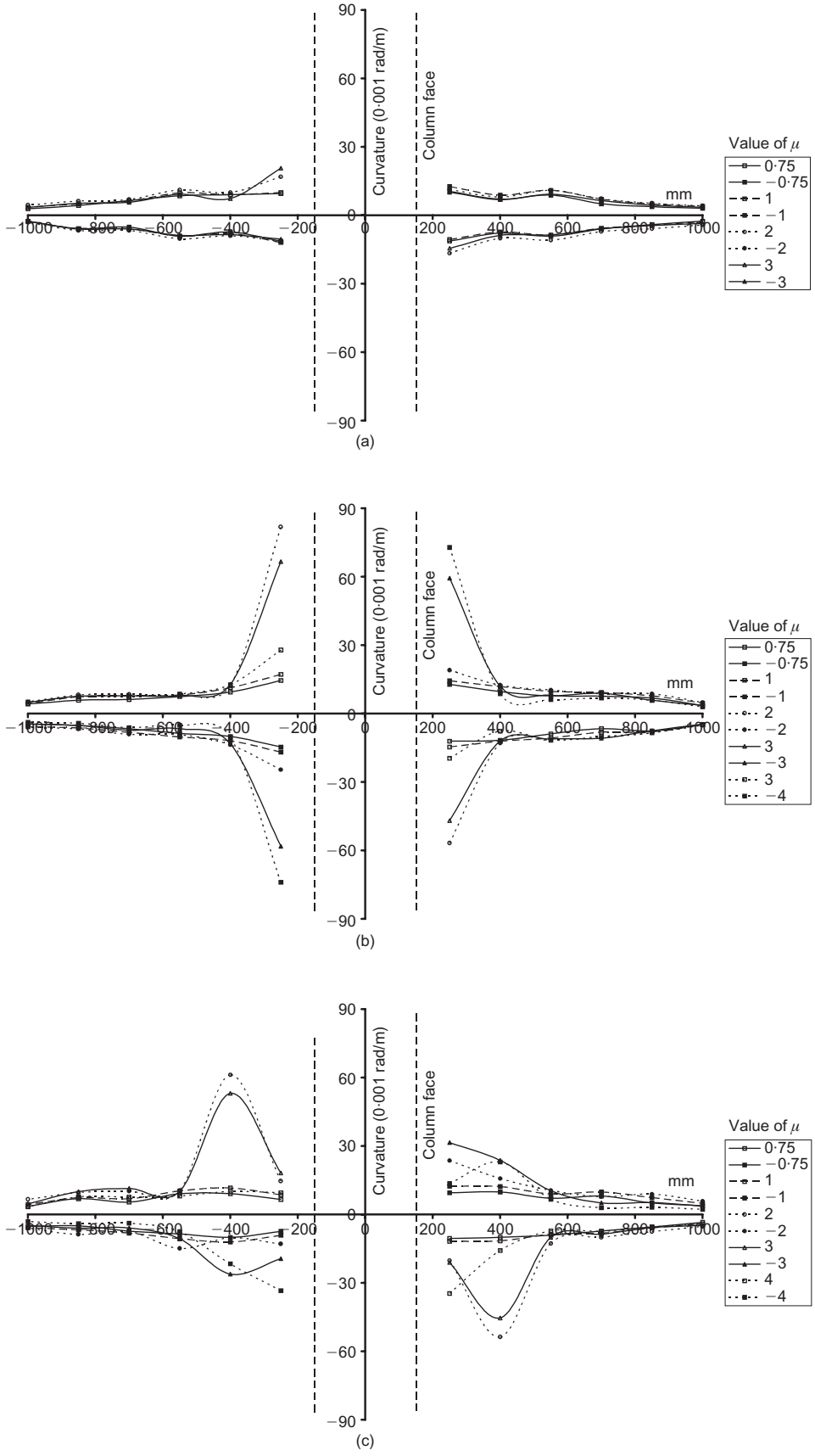

Fig. 14. Curvature profile along the beam: (a) unit E-0·0; (b) unit H-0·0; (c) unit AD-0·0

column interface. It also suggested that large bending deformations and therefore damage took place in the vicinity of the beam–column joint. The profiles for unit AD-0·3 are different from the rest in that the plastic hinge occurred at a distance outside the joint. The presence of the diagonal bars strengthened both the joint itself as well as a short length of the beam adjacent to the joint, thus shifting the location of plastic hinges away from the critical joint region. An RC frame

with beam–column joints reinforced with diagonal bars is therefore more repairable. As opposed to those of units E-0·3 and H-0·3, the high beam curvatures for unit AD-0·3 were distributed over a length of the same order as the beam depth. The full development of plastic hinges without the hindering effects of the beam–column joint enables better exploitation of the rotational capacity of the beam in energy absorption during earthquakes. It also agrees well with the design philosophy of strong columns and weak beams, according to which the strength and inelastic deformation capacity of a structure are governed by flexural yielding at plastic hinges at preferred locations in the beams and the ground storey columns. Provided that the capacity design rationale[4] is followed and realistic flexural capacities of the beams are used, reasonable safety of the structure during an earthquake can be ensured. This is also confirmed by the experiments throughout which the columns remained essentially elastic with comparatively minor cracking.

4.7. Bond stresses of beam reinforcement within joint

The bond slip of the longitudinal reinforcing bars of the beam within the beam–column joint is recognised as one major cause for stiffness degradation, and it shows up in the pinching of the load-displacement hysteretic loops. Under lateral seismic loading, the beam bending moments acting on the two sides of a beam–column joint are of the opposite sense. For a longitudinal reinforcing bar going through the joint, one end is in compression while the other is in tension. This typical 'push–pull' situation is undesirable as it sets up high bond stresses within the joint. These bars will sooner or later suffer from bond-slip under inelastic reversed cyclic loading. Similar consideration of the diagonal bar as shown in the inset of Fig. 4(c) concludes that the bar is in either the 'push–push' or 'pull–pull' situation, which requires little bond resistance along the diagonal part within the joint. In specimens of the AD-series, part of the forces carried by the longitudinal bars in the beam are transferred to the diagonal bars through the development length outside the joint, thereby relieving the bond stresses along these longitudinal bars within the joint.

Measurements from strain gauges attached on the top longitudinal bars in the beam were analysed for each specimen. Figure 15 shows the peak values of each loading cycle for units E-0·0, H-0·0 and AD-0·0. Also plotted for reference is the value of yield strain. The peaks in the figure are associated with cracks in the vicinity. Most of these strains were tensile due to the large residual strains resulting from inelastic reversed cyclic loading. Within the width of the column, the strains of the top beam bars in unit E-0·0 were larger than the others, suggesting yield penetration and bond slip. The slightly lower strains of the top beam bars in unit H-0·0 indicated that the nominal hoops did help to relieve the bond demand. The peaks of strain outside the joint also showed that a certain degree of plastic bending took place in the beam. In the presence of the diagonal bars, the strains of the top beam bars in unit AD-0·0 were kept relatively low and therefore the bond stresses there were more favourable. The high peaks of strain in the beam further away from the joint demonstrated that the plastic hinges were shifted away from the joint and well developed.

The bond stresses along longitudinal bars, both in the beam and column, played an important role in the shear behaviour of the joint, not only because the shear force was introduced to the joint through bond stresses but also because the bond condition influenced the apportionment of resistance between the internal shear mechanisms directly.[15] Yield penetration of beam reinforcement usually leads to loss of bond between the reinforcing bars and the surrounding concrete in the joint. The bond deterioration will likely diminish the contribution of the compression zone that activates the concrete strut and it further reduces the stiffness of the joint.

4.8. Contribution from diagonal bars to shear resistance of joint

In section 3·1 the equivalent reinforcement area required for the diagonal bars has been taken to be 70% of that of the normal transverse reinforcement. Therefore it is necessary to confirm whether this figure is reasonable or not. Table 4 summarises a number of parameters that reflect the effectiveness of various joint details, namely the effective horizontal area of joint reinforcement A_{sh}, the measured equivalent shear strength of the column V_{max}, the nominal shear strength of the column derived from the nominal flexural strength of the beam V_n, the maximum joint shear V_{jh} as in section 4·1, the shear taken by the joint reinforcement and the shear taken by the concrete. In particular, the effective horizontal area of joint reinforcement for the H-series is simply the cross-sectional area of hoops and crossties within the joint. For the AD-series, it is observed from the experiments that both sets of diagonal bars have yielded at the maximum loading. For this case, the effective horizontal area is therefore taken as that giving the same force as the total horizontal component of those taken by the diagonal bars when they have yielded. The shear taken by the joint reinforcement is the horizontal shear force at the joint estimated from the strain readings, whereas the shear taken by the concrete is taken as the difference between the maximum joint shear V_{jh} and the shear taken by joint reinforcement.

In the design of the joint reinforcement for specimens in the H- and AD-series, the joint reinforcement provided is actually more than the calculated minimum requirement. To investigate the scenarios if such minimum joint reinforcement is provided, hypothetical specimens H-0·0*, AD-0·0*, H-0·3* and AD-0·3* are considered. For example, the results for the hypothetical unit AD-0·0* (with the minimum joint reinforcement) are obtained by interpolation between those of E-0·0 (with no joint reinforcement) and those of AD-0·0 (with joint reinforcement above the minimum). When no column axial load is present, only units AD-0·0 and AD-0·0* can develop a column shear strength V_{max} above the nominal column shear strength V_n. When column axial load is present, units of the H- and AD-series can all achieve this. Based on the shear taken by the concrete calculated by this simplistic approach, it can be seen that the provision of diagonal bars actually enhances the ability of the joint concrete to take shear. For example, the shear forces taken by the concrete in the units of the AD-series are all above the respective values in the corresponding empty joints of the E-series. Therefore the 70% assumption in deriving equation (5) is justified.

5. CONCLUSION

Six half-scale interior beam–column assemblies with different joint details, namely 'empty', nominal transverse reinforcement

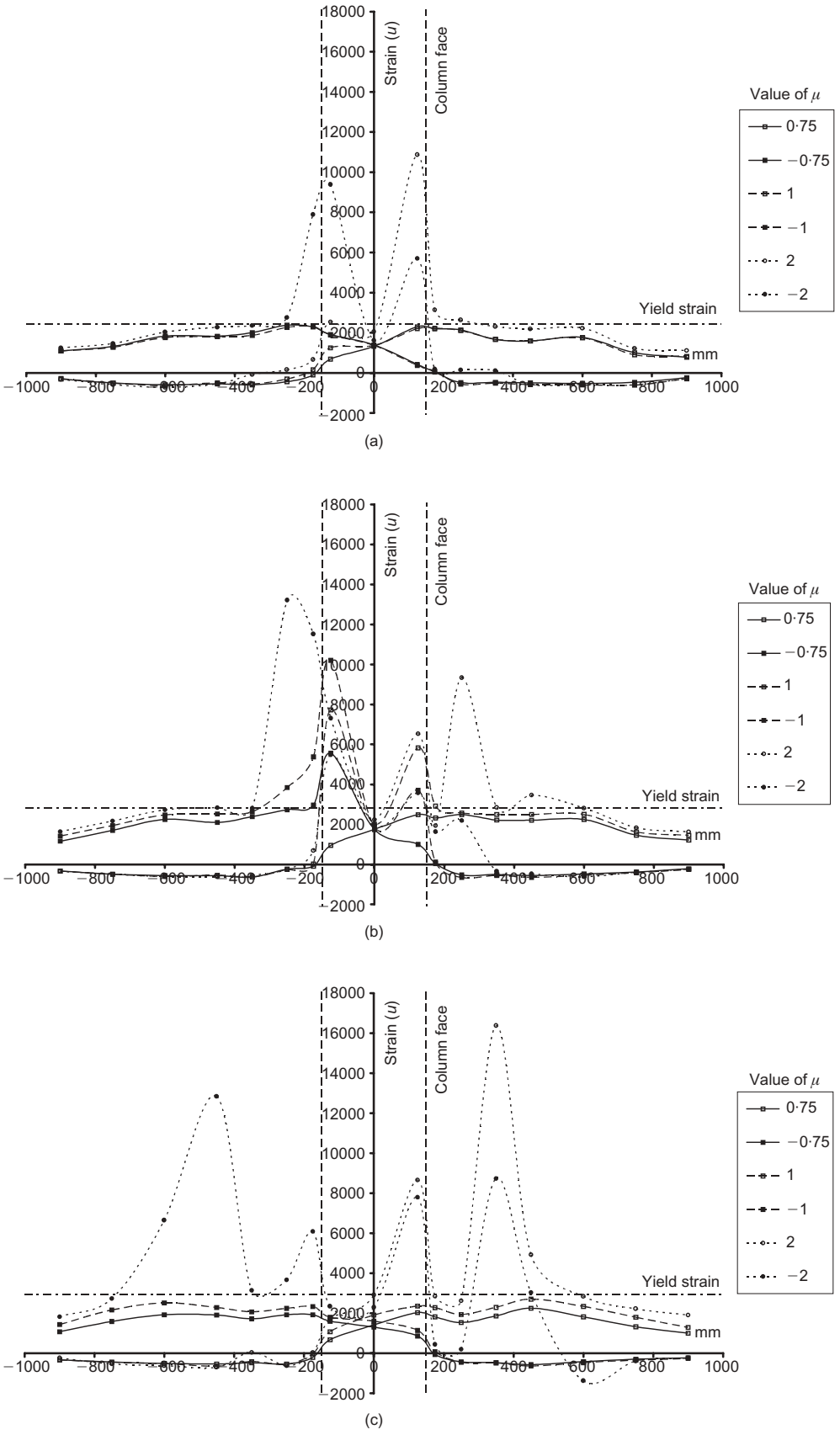

Fig. 15. Strain distribution at top beams bats: (a) unit E-0·0; (b) unit H-0·0; (c) unit AD-0·0

and diagonal bars, tested under reversed cyclic loading are reported in this paper. Within each pair of specimens with identical detailing, compressive column axial load was applied to one of them while the other one was tested without column axial load. The internal forces and stresses were estimated from experimental measurements, actual material properties where possible and the basic principles of structural mechanics. Although scale effects and deviations in the results due to the

Unit	Effective A_{sh}: mm^2	Measured V_{max}: kN	Nominal V_n: kN	Max. joint shear V_{jh}: kN	Shear taken by joint reinft.: kN	Shear taken by concrete: kN
E-0·0	–	78·9	85·5	750·4	–	750·4
H-0·0	1018	90·2	99·2	869·3	462·4	406·9
AD-0·0	569	95·6	92·9	1175·5	234·8	940·7
H-0·0*	683	86·5	94·7	830·2	310·2	520·0
AD-0·0*	478	92·9	91·7	1107·5	197·2	910·3
E-0·3	–	88·9	93·1	813·9	–	813·9
H-0·3	1018	91·0	86·6	743·9	418·9	325·0
AD-0·3	569	98·0	89·4	1049·2	227·3	821·9
H-0·3*	683	90·3	88·7	766·9	281·0	485·9
AD-0·3*	478	96·5	90·0	1011·6	190·9	820·7

A specimen name with asterisk is a hypothetical one with minimum required amount of joint reinforcement.
Results based on interpolation are shown in italics.

Table 4. Effectiveness of joint reinforcement

adopted experimental procedures cannot be ruled out entirely, they are not considered significant as the present work is built on well-established principles of internal equilibrium of the adjacent members. From the above experimental results, which are further confirmed by other units tested in the research project, the following conclusions are drawn.

(*a*) The 'empty' beam–column joint has the least strength and its strength sustainability is also inferior to the other two methods of detailing. The 'empty' joint is therefore not suitable even under moderate seismicity.
(*b*) Beam–column joints reinforced with diagonal bars performed better than those reinforced with nominal hoops in terms of strength and stiffness degradation at lower ductility factors. However, at high ductility factors, the former specimens experienced more strength and stiffness degradation compared to the latter specimens.
(*c*) Strength enhancement occurred in the units containing diagonal bars whether or not column axial load is present, while it occurred in the unit containing nominal hoops only in the presence of compressive axial load. However, for the identical unit containing nominal hoops without compressive axial load, it could hardly reach the theoretical ultimate strength.
(*d*) The presence of diagonal bars resulted in improvement of the bond condition within the joint and helped to control the development of the beam–column interface cracks, all of which contributed in effectively maintaining the stiffness of the overall assembly.
(*e*) Interior beam–column joints reinforced with diagonal bars perform fairly satisfactorily at lower ductility factors while it can ease the congestion of steel in the joint region. The proposed detailing with diagonal bars is therefore suitable for joints of RC frame structures located in low to medium seismic regions.

6. ACKNOWLEDGEMENTS

The work described in this paper has been substantially supported by the Research Grants Council of the Hong Kong Special Administrative Region, China (RGC Project No. HKU 7012/00E). Technical support provided by the laboratory staff of the Department of Civil Engineering, The University of Hong Kong is gratefully acknowledged. The authors are also grateful to the constructive comments from the assessor.

REFERENCES

1. Lee D. L. N., Wight J. K. and Hanson R. D. RC beam–column joints under large load reversals. *Journal of the Structural Division, ASCE*, 1977, **103**, No. 12, 2337–2350.
2. Durrani A. J. and Wight J. K. Behavior of interior beam-to-column connections under earthquake-type loading. *ACI Journal*, 1985, **82**, No. 3, 343–349.
3. Cheung P. C., Paulay T. and Park R. Behavior of beam–column joints in seismically-loaded RC frames. *The Structural Engineer*, 1993, **71**, No. 8, 129–138.
4. Park R. and Paulay T. *Reinforced Concrete Structures*. Wiley, New York, 1975.
5. Building Authority. *Code of Practice for the Structural Use of Concrete*. Building Authority, Hong Kong, 1987.
6. British Standards Institution. *Structural Use of Concrete, Code of Practice for Design and Construction*. BSI, Milton Keynes, 1997, BS 8110: Part 1.
7. Standards New Zealand. *New Zealand Standards – Part 1: The Design of Concrete Structures*. SNZ, Wellington, 1995, NZS 3101.
8. ACI-ASCE Committee 352. *Recommendations for Design of Beam–Column Joints in Monolithic Reinforced Concrete Structures*. ACI, Detroit, MI, 1991.
9. Tsonos A. G., Tegos I. A. and Penelis G. G. Seismic resistance of type 2 exterior beam-column joints reinforced with inclined bars. *ACI Structural Journal*, 1992, **89**, No. 1, 3–12.
10. Pam H. J., Au F. T. K., Huang K. and Li J. Behaviour of interior beam–column joints reinforced with diagonal steel for moderate seismicity level. *Proceedings of the Structural Engineers World Congress SEWC2002*, 9–12 October 2002, Yokohama, Japan, Paper T1-3-d-5, 8 pp.
11. Leon R. T. Shear strength and hysteretic behavior of interior beam-column joints. *ACI Structural Journal*, 1990, **87**, No. 1, 3–11.
12. Hakuto S., Park R. and Tanaka H. Seismic load tests on interior and exterior beam–column joints with substandard reinforcing details. *ACI Structural Journal*, 2000, **97**, No. 1, 11–25.
13. Collins M. P. and Mitchell D. A rational approach to shear design. *ACI Journal*, 1986, **83**, No. 6, 925–933.
14. British Standards Institution. *Eurocode 8: Design Provisions for Earthquake Resistance of Structures, Part 1·3 General Rules – Specific Rules for Various Materials*

and Elements. BSI, Milton Keynes, 1996, DD ENV 1998-1-3:1996·17

15. POPOV E. P. Bond and anchorage of reinforcing bars under cyclic loading. *ACI Journal*, 1984, **81**, No. 4, 340–349.

Please email, fax or post your discussion contributions to the secretary by 1 August 2005: email: journals@ice.org.uk; fax: +44 (0)20 665 2294; or post to Journals Department, Institution of Civil Engineers, 1–7 Great George Street, London SW1P 3AA.